

<https://doi.org/10.1038/s42003-025-08219-0>

Two neuropeptide signaling pathways regulate post-mating refractoriness and reproductive system in male crickets



Zhen Zhu & Shinji Nagata

After mating, some insects drastically reduce mating activity, termed post-mating refractoriness, due to physiological restrictions. Male crickets, *Gryllus bimaculatus*, characteristically exhibit a 1-hour post-mating refractory stage, which is controlled by terminal abdominal ganglion. The molecular mechanisms underlying the male-specific precisely timed refractory stage remain unclear. Here, we show that among 28 neuropeptide precursors expressed in the terminal abdominal ganglion, *myosuppressin*, *allatotropin*, and *sNPF* exhibited male-specific expression based on RT-qPCR and in situ hybridization. RNA interference experiments showed that only the knockdown of *allatotropin* and *sNPF* extended the refractoriness duration. Furthermore, *allatotropin* and *sNPF* knockdown influenced the male reproductive system by inhibiting seminal fluid secretion from the male accessory gland and decreasing spermatozoon storage in seminal vesicles, respectively. Knockdown of *allatotropin* and *sNPF* receptors caused similar phenotypes to their ligands. In conclusion, this study demonstrated the regulation of post-mating refractoriness and reproductive system by Allatotropin and sNPF signaling pathways in male crickets.

In polygamous insects, multiple matings benefit the fecundity and fertility of the population¹. Females with experience of multiple matings are guarded by more mating partners and protected against male infertility, and replenish the depleted sperm stores^{2,3}. Additionally, multiple matings contribute to male competition for fertilization success⁴. Despite these advantages, the energy consumption of mating restricts continuous mating behavior in most cases. Therefore, immediately after mating, insects enter a refractory stage (RS) during which they show no mating activity and replenish the energy and gametes consumed in the previous mating. The duration of the post-mating refractoriness limits the mating frequency. Extensive research has focused on the regulatory mechanisms underlying post-mating refractoriness in females. Female insects typically receive special substances from males, such as sex peptide from the male fruit fly *Drosophila melanogaster* and a male-specifically modified steroid, 3-dehydro-20-hydroxyecdysone from the male mosquito, *Anopheles gambiae*, during copulation^{5,6}. These male-derived substances activate downstream signaling in females to reduce receptivity to remating, leading to post-mating refractoriness. In contrast, much less attention has been given to understanding the mechanisms underlying post-mating refractoriness in male insects.

Crickets, belonging to the Grylloidea insect superfamily, serve as excellent models for studying male post-mating refractoriness due to their

identifiable reproductive cycle which is composed of mating stage and post-mating RS. The mating stage initiates with a calling or courtship song and ends with spermatophore extrusion, while the RS begins with spermatophore extrusion and extends to the onset of next calling or courtship songs⁷ (Fig. 1). Crucially, different from the female refractoriness, whose duration changes with the accumulation of male-derived substances⁸, the RS of male crickets is precisely timed⁹. This stage can be further compartmentalized into RS1, which is from the extrusion of the old spermatophore to the protrusion of a new immature spermatophore, and RS2, which is from spermatophore protrusion to the onset of calling or courtship songs (Fig. 1). In the case of the two-spotted cricket, *Gryllus bimaculatus*, although the duration of RS1 is susceptible to internal and external influences, it typically lasts for approximately 6 min under normal conditions in the presence of females¹⁰. The duration of RS2 in *G. bimaculatus* is constantly 1 h¹¹. The clock timer governing the RS2 has been identified in the terminal abdominal ganglion (TAG), located at the end of the central nervous system in crickets¹². However, the molecular mechanisms underlying the precisely timed post-mating refractoriness remain largely unknown.

Neuropeptides are the largest group of critical signaling molecules that orchestrate various physiological and behavioral activities, including reproduction in animals¹³. To date, few descriptions of the regulation of reproductive behaviors in male insects by neuropeptides have been

Department of Integrated Biosciences, Graduate School of Frontier Sciences, the University of Tokyo, 5-1-5 Kashiwanoha, Kashiwa, Chiba, Japan.

✉ e-mail: shinjin@edu.k.u-tokyo.ac.jp

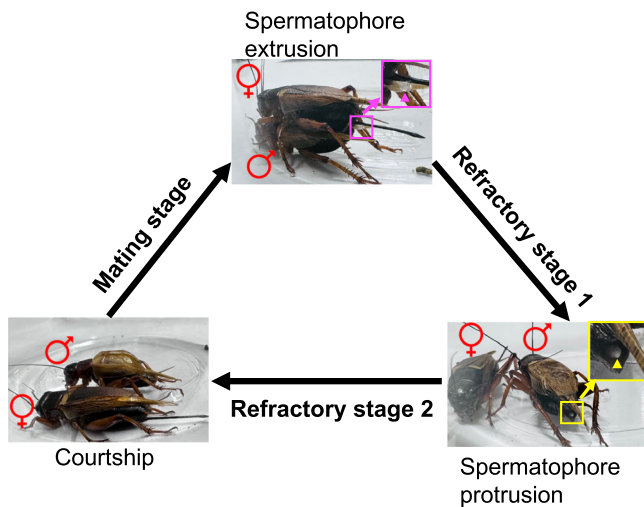


Fig. 1 | The male reproductive cycle of *G. bimaculatus*. Mating stage is from calling or courtship observed by wing vibration to spermatophore extrusion of males. The magenta rectangle region is enlarged. A magenta triangle points toward the spermatophore that is extruded from the male and attached to the external genitalia of the mated female. Refractory stage is further divided into refractory stage 1 (RS1) and refractory stage 2 (RS2). RS1 is from spermatophore extrusion to the protrusion of a new immature spermatophore which is enlarged and pointed by a yellow triangle. RS2 is from spermatophore protrusion to the onset of calling or courtship.

reported^{14–18}. We here sought to decipher whether TAG-derived neuropeptides were involved in regulating the precisely timed male post-mating refractoriness and explore their functions.

In the present study, we identified 28 neuropeptide precursors expressed in the TAG. Two neuropeptides, *allatotropin* (AT) and *short neuropeptide F* (*sNPF*), contributed to the precisely timed male post-mating refractoriness. Additionally, the two neuropeptides regulated the physiological activities in the male reproductive system that are essential for spermatophore preparation. Specifically, knockdown of AT signaling pathway suppressed secretion of seminal fluid from the male accessory gland, while knockdown of *sNPF* signaling pathway inhibited spermatozoon storage in the seminal vesicles. In summary, our findings provide new insights into the mechanisms underlying the male post-mating refractoriness and spermatophore preparation in the male reproductive system.

Results

Myosuppressin, AT, DH31, and *sNPF* exhibit male-specific expression in the TAG

To investigate the regulation of male-specific, precisely timed post-mating refractoriness by neuropeptides in crickets, we first explored the neuropeptides with sexually different expression. TAGs were dissected from male adults on the fourth day after eclosion, as the crickets reached sexual maturation by this time, followed by RNA sequencing analysis. Data by RNA sequencing analysis identified the expression of 28 neuropeptide precursors in the male TAG. To determine which of these neuropeptides exhibited male-specific expression in the TAG, we dissected both male and female TAGs for subsequent RT-qPCR and in situ hybridization. RT-qPCR unveiled that 4 of 28 neuropeptide precursors exhibited sexually different expression in the TAGs (Fig. 2); *Adipokinetic hormone/corazonin-related peptide* showed lower expression in the male TAG than in the female TAG, whereas *myosuppressin*, AT, and *sNPF* exhibited significantly higher transcriptional levels in the male TAG compared to the female TAG (Fig. 2). The developmental distribution analyses showed that the sexual differences in the transcriptional levels of *myosuppressin*, AT, and *sNPF* precursors were observed from the penultimate instar, when the expression of the three precursors increased in the male TAG but did not alter in the female TAG, suggesting their involvement in regulating male-specific events from this

developmental stage. Moreover, AT displayed an additional increase in expression at the adult stage, and *sNPF* exhibited a similar trend, implying potential roles in male adult behaviors and physiological activities (Fig. 3a–c and Supplementary Fig. 1).

Subsequently, whole-mount in situ hybridization revealed the locations of the positive cells expressing the neuropeptide precursors. Among 17 neuropeptide precursors with successfully detected signals, *myosuppressin*, AT-, *sNPF*-, and *diuretic hormone 31* (DH31)-expressing cells in the TAG exhibited sexual difference (Fig. 4). The positive cells of *myosuppressin*, AT, and *sNPF* in the male TAG were noticeably more than those in the female TAG, consistent with the higher transcript abundance in the male TAG as showed in the RT-qPCR results (Fig. 2). The expressing cells of *myosuppressin*, AT, *sNPF*, and DH31 were similarly distributed in the dorsal midline of the male TAG, forming two nervous cell clusters at the posterior median and bottom median regions. In contrast, no comparable signals were observed in these regions of the female TAG (Fig. 4). In fact, DH31-expressing cells were predominantly distributed in the ventral and bilateral regions but not dorsal region, which was observed both in the male and female TAGs (Fig. 4). The difference in the expression in the dorsal TAG might be too small to be detected by RT-qPCR, explaining the comparable DH31 transcriptional levels in the male and female TAGs at all developmental stages (Figs. 2, 3d, and 4). These findings collectively suggest that the four male-specifically expressing neuropeptides may possess pivotal roles in male-specific behaviors and physiological activities.

AT and *sNPF* signaling pathways regulate the duration of male post-mating refractoriness

Knockdown experiments using RNA interference (RNAi) were conducted to investigate the contributions of *myosuppressin*, AT, *sNPF*, and DH31 to post-mating refractoriness in male crickets. RNAi was efficient for loss-of-function analyses of these four genes (Supplementary Fig. 2a–d). The number of matings completed in 12 h and the duration of each post-mating RS were recorded. During 12 h of observation period, DH31 knockdown males exhibited courtship behavior but failed to transfer spermatophores to females. These males with failed mating continued courting and did not enter post-mating RS. Consequently, the effects of DH31 on the RS duration could not be evaluated. *Myosuppressin* knockdown males averagely experienced 10.4 matings in 12 h experiment, which was comparable to that of the control males with 11.2 matings (Fig. 5a). Little difference in the duration of RSs was observed between *myosuppressin* knockdown crickets and the control (Fig. 5b). Conversely, AT and *sNPF* knockdown males experienced 9.4 and 8.7 matings, respectively, significantly fewer than the control males (Fig. 5a), and exhibited a significant increase in RS duration, with average extensions of 8.5 and 9.5 min, respectively (Fig. 5c, d). These results demonstrated that AT and *sNPF* knockdown males mated at a lower frequency. The RNAi targeting AT receptor (ATR) and *sNPF* receptor (*sNPF*R) reduced the mating frequency to 8.4 and 8.3 matings, respectively, significantly fewer than the 10 matings observed in the control males. Additionally, the RS duration was significantly decreased by 15.2 and 11.5 min, respectively (Supplementary Fig. 2e, f; Fig. 5e–g). As both AT and *sNPF* were found to regulate post-mating refractoriness, we next investigated whether these two neuropeptides functionally interacted. Single knockdown of AT or *sNPF*, as well as simultaneous knockdown of AT and *sNPF*, reduced the number of matings and extended the RS duration. However, the simultaneous knockdown did not cause any additional or synergistic effects on the male post-mating refractoriness compared to single knockdowns (Supplementary Fig. 3). Moreover, AT knockdown did not alter the transcriptional level of *sNPF* in the TAG, and *sNPF* knockdown had no effect on the transcriptional level of AT in the TAG (Supplementary Fig. 2b, c), suggesting that AT and *sNPF* might not be the downstream signaling molecules of each other. Therefore, it is likely that AT and *sNPF* regulate the post-mating refractoriness in male crickets in parallel through different targets of signaling pathways.

Most orthoptera species prepare a new spermatophore in the male reproductive system for the subsequent matings during the RS. In crickets,

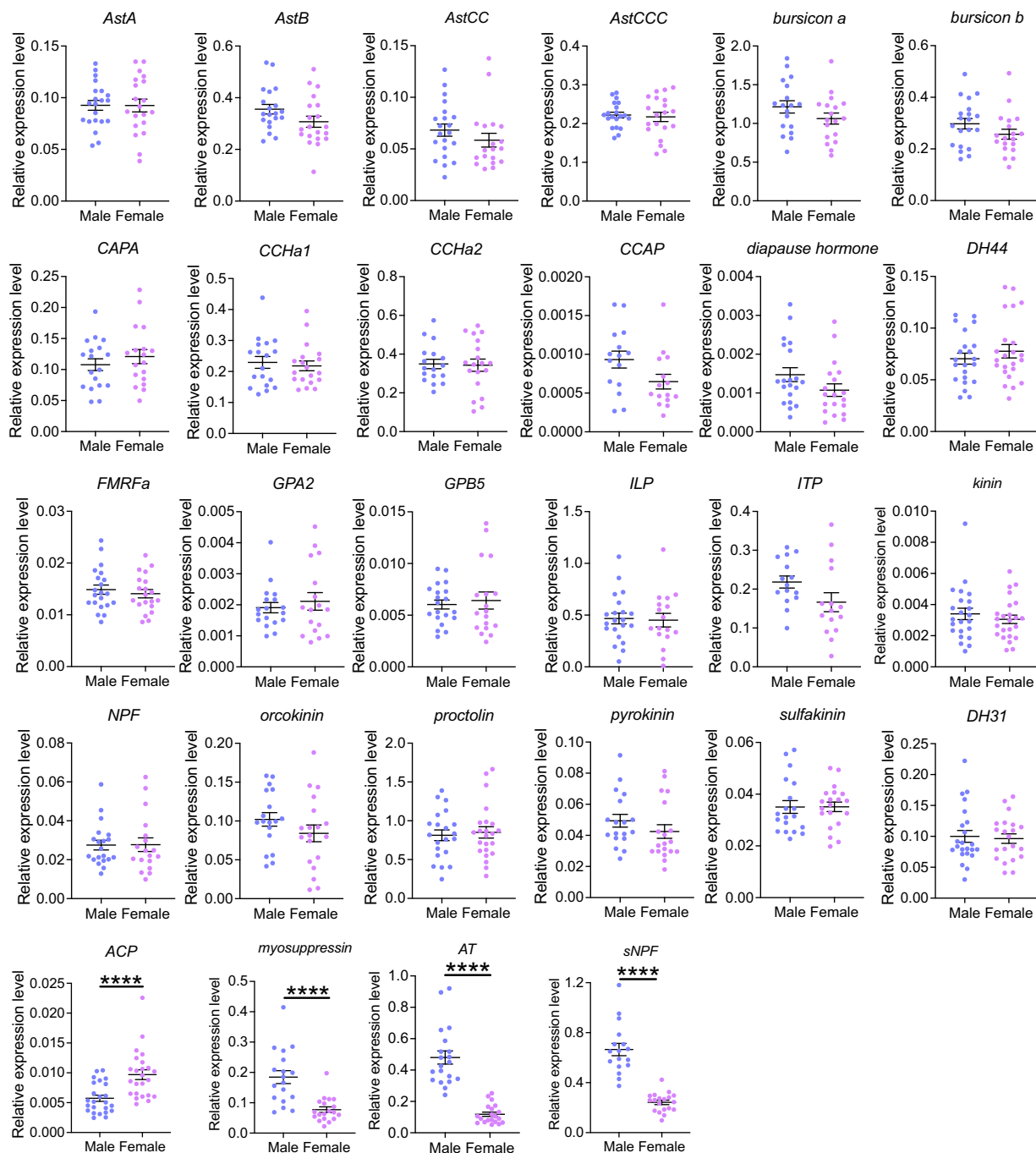


Fig. 2 | Transcriptional levels of neuropeptide precursors in male and female TAGs. The TAGs were dissected from male and female crickets on the fourth day after eclosion. Values are shown as mean \pm SEM, $n = 15\text{--}24$, unpaired t -test, **** $P < 0.0001$. AstA, allatostatin A. AstB, allatostatin B. AstCC, allatostatin CC. AstCCC, allatostatin CCC. CAPA, capability. CCHa1, CCHamide1. CCHa2,

CCHamide2. CCAP, crustacean cardioactive peptide. DH44, diuretic hormone 44. GPA2, glycoprotein alpha 2. GPB5, glycoprotein beta 5. ILP, insulin-like peptide. ITP, ion transport peptide. NPF, neuropeptide F. DH31, diuretic hormone 31. ACP, adipo-kinetic hormone/corazonin-related peptide. AT, allatotropin. sNPF, short neuro-peptide F.

spermatophore materials, including seminal fluid from the male accessory gland (MAG) and spermatozoa from the seminal vesicles (SVs), are transported to the subgenital plate, where these materials are assembled into a mature capsule-like spermatophore¹⁹. Although previous studies suggest that the duration of the process of spermatophore preparation is a potential determinant of the duration of post-mating refractoriness in insects^{20,21}, this seems not to be the case in crickets. We removed MAG/SVs complex from the male adults on the first day after eclosion, preventing the males from preparing spermatophores after sexual maturation. These

MAG/SV-ablated males exhibited comparable RS duration to the control (Supplementary Fig. 4). This suggests that AT and sNPF regulate the refractoriness independently of spermatophore preparation, including the process of transport of seminal fluid and spermatozoa from MAG/SVs, in crickets. In *D. melanogaster*, silencing *ecdysis-triggering hormone receptor* in the sole juvenile hormone (JH)-producing tissue, corpus allatum, reduces post-mating refractoriness in male flies, which can be partially restored by JH analog application²². However, injection of a JH analog, fenoxycarb, at various doses into crickets did not alter RS duration

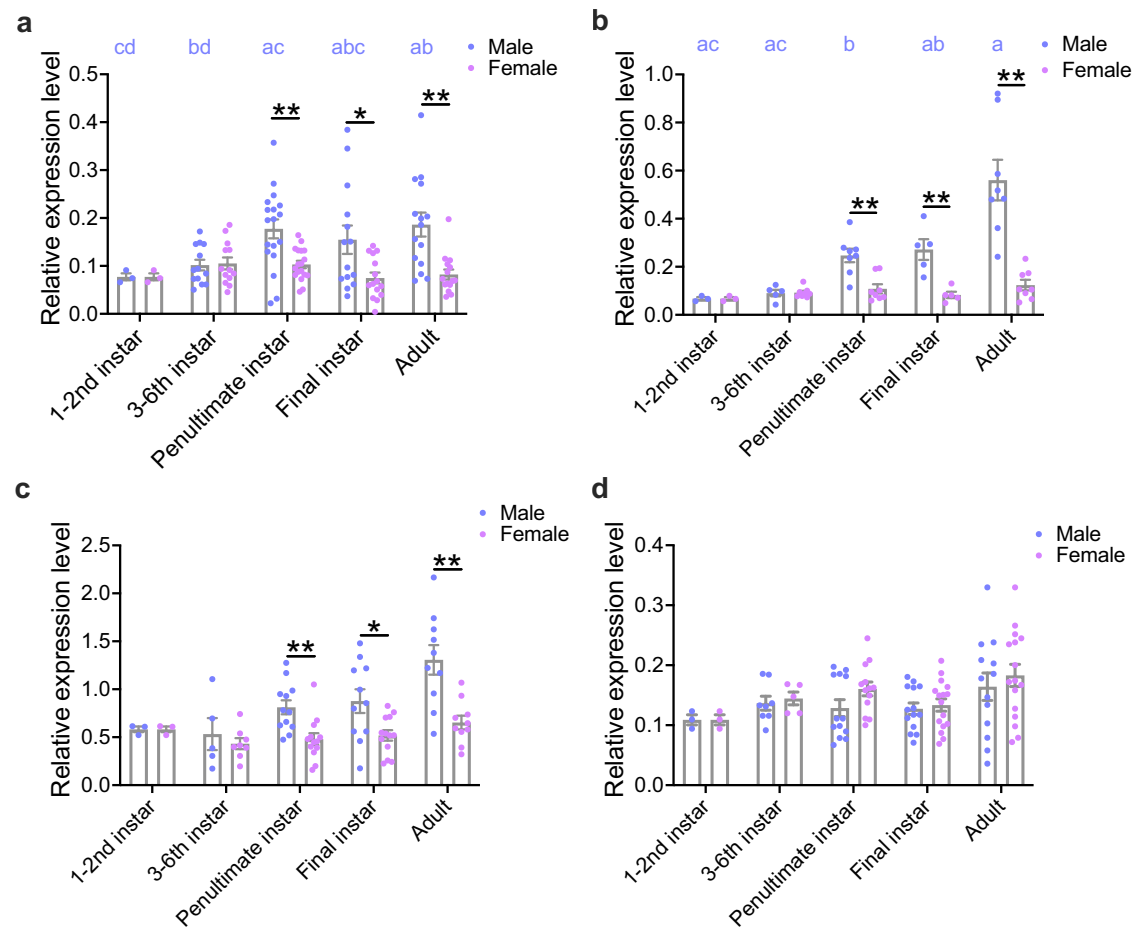


Fig. 3 | Transcriptional levels of the neuropeptides in the TAGs of male and female crickets at different growth stages. a *myosuppressin*. **b** *AT*. **c** *sNPF*. **d** *DH31*. Values are shown as mean \pm SEM. 1–2nd instar, $n = 3$ batches, 40–50 crickets/batch. 3–6th instar, $n = 5$ –13 batches, 5–10 crickets/batch. Penultimate instar, $n = 8$ –18 batches, 3 crickets/batch. Final instar, $n = 5$ –16 batches, 2 crickets/

batch. Adult, $n = 8$ –17 batches, 2 crickets/batch. Tukey's test. Asterisks represent significant differences between sexes. * $P < 0.05$, ** $P < 0.01$. Different letters represent significant differences among male developmental stages. The morphological characteristics used to separate growth stages are detailed in Supplementary Fig. 1.

(Supplementary Fig. 5), suggesting the little effect of JH on the post-mating refractoriness in crickets.

We noticed that the RS duration increased after successively multiple matings (Fig. 5b and Supplementary Fig. 6a). The transcriptional responses of AT/ATR and sNPF/sNPF_R signaling pathways to multiple matings were examined. The transcriptional level of AT in the TAG decreased with multiple matings, while no alteration in sNPF expression in the TAG was observed (Supplementary Fig. 6b, c). However, changes in the secretion level of sNPF peptide cannot be ruled out. Since the physiological activities in the MAG and SVs were not required for maintaining the RS (Supplementary Fig. 4), AT and sNPF likely act on other tissues, such as the brain, which controls stridulatory behavior necessary for courtship^{23–25}. The transcriptional levels of *ATR* and *sNPF_R* in the brains of RNAi crickets were measured using RT-qPCR to assess RNAi efficiency. Their expression levels were significantly reduced by RNAi, indicating that the dysfunctional ATR and sNPF_R in the brain might contribute to the altered RS duration (Supplementary Fig. 2e, f). A slight increase in the transcriptional levels of *ATR* and *sNPF_R* was observed in the brains of the multiply mated males compared to the virgins (Supplementary Fig. 6d, f), indicating the potential involvement in feedback regulation.

We next examined whether AT and sNPF with similar effects on the male post-mating refractoriness were colocalized in the male TAG. Double-staining using immunohistochemistry for AT and in situ hybridization for sNPF were performed. The specificity of AT antiserum was confirmed by dot blotting assay, preadsorption assay and colocalization of AT peptide and

AT mRNA (Supplementary Fig. 7). AT peptide and sNPF mRNA were colocalized in the large cells with a diameter of around 40 μ m in the posterior region and bottom region of the dorsal midline of the male TAG (Fig. 5h). These cells co-expressing AT and sNPF in the male TAG may be responsible for concomitant regulation of the post-mating refractoriness by AT and sNPF. Additionally, in the same regions, AT peptide was specifically distributed in a group of smaller cells with a diameter of around 15 μ m, while sNPF was specifically expressed in two other small cells with similar diameters (Fig. 5h). The different distributions of AT and sNPF in these small cells indicate that the two neuropeptides may have distinct functions, despite their concomitant regulation of the male refractoriness. Notably, the neurons expressing these neuropeptides in the male TAG seemed to be the male-specific neurons directly innervating the reproductive tissues in crickets, as they were distributed in the dorsal posterior median regions²⁶. Consequently, an arising question was whether AT and sNPF, expressed in different small cells in the male TAG, regulated the functions of distinct reproductive tissues.

AT and sNPF target different sites within the male reproductive system

The male reproductive system in crickets encompasses testes, vasa deferentia, SVs, MAG, and ejaculatory duct (Fig. 6a). These reproductive tissues, innervated by TAG^{27,28}, play distinct roles in spermatophore preparation during the post-mating RS²¹. To investigate whether AT and sNPF were involved in specific processes of spermatophore preparation, we explored

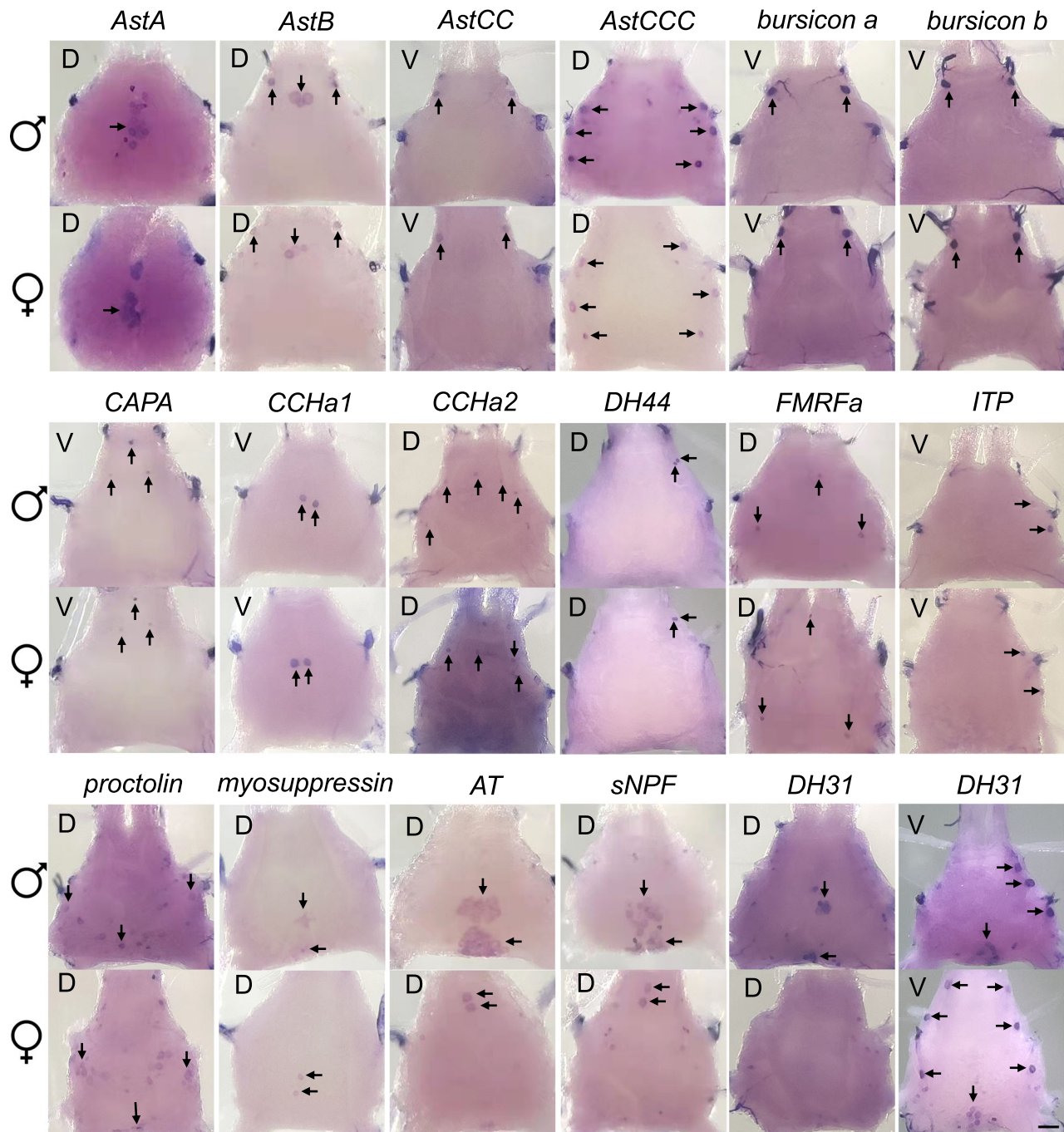


Fig. 4 | Distributions of neuropeptide-expressing cells in male and female TAGs examined by whole-mount in situ hybridization. In situ hybridization was performed at least twice for each gene. In each experiment, five samples were analyzed. Arrows point to the positive cell. D, dorsal side, V, ventral side. Bar, 100 μ m.

the target tissues of AT and sNPF by examining the spatial distributions of *ATR* and *sNPF* in the male reproductive system of the sexually mature male crickets. *ATR* exhibited the highest transcriptional level in the MAG, whereas the highest transcriptional level of *sNPF* was observed in the vasa deferentia and SVs (Fig. 6b, c). The spatial difference in *ATR* and *sNPF* expression in the male reproductive system indicated the specific regulatory roles of the two signaling pathways in the process of spermatophore preparation. Considering the innervation of MAG and SVs by TAG, it was asked whether AT and sNPF functioned as neurotransmitters to regulate these reproductive tissues. Direct matrix-assisted laser desorption/ionization time-of-flight mass spectrometry (MALDI-TOF MS) revealed that the mature peptides of AT and sNPF with theoretical m/z 1366.6 and 1331.8,

respectively, were detected in the TAG-MAG/SV nerves (Supplementary Fig. 8a), indicating their roles as neurotransmitters.

The MAG of crickets emerged at the 3rd instar. From the 3rd instar to the early final instar, the MAG exhibited a morphology resembling a semitransparent faba bean. A significant morphological transformation was observed from the final instar to the adult stage. A substantial number of short or long, slender, blind-ending tubules protruded from the base of MAG (Supplementary Fig. 9a). Interestingly, the transcriptional levels of *ATR* in the MAG and *AT* in the TAG increased concomitantly with development. A notable surge was observed from the final instar to the adult stage (Supplementary Fig. 9a). This observation aligned with the period when the MAG underwent a drastic morphological change (Supplementary

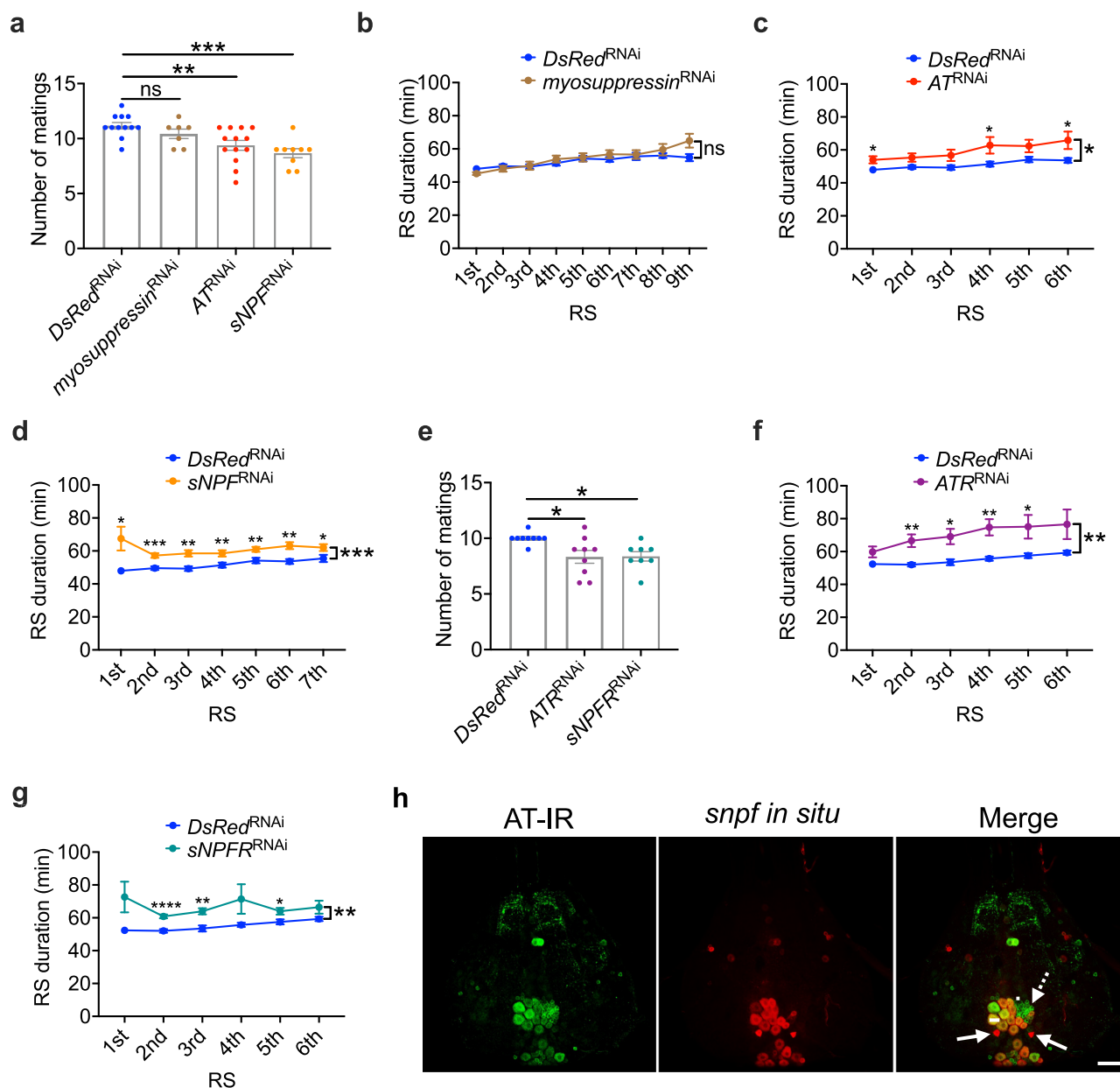


Fig. 5 | Regulation of male post-mating refractoriness by neuropeptide signaling pathways. **a** Numbers of matings of male crickets injected with *dsDsRed* (*DsRed^{RNAi}*), *dsmyosuppressin* (*myosuppressin^{RNAi}*), *dsAT* (*ATR^{RNAi}*), or *dsNPFR* (*sNPFR^{RNAi}*) in 12 h. Values are shown as mean \pm SEM, $n = 7-13$, Dunnett's test, ** $P < 0.01$, *** $P < 0.001$. ns, not significant. **b–d** Duration of each RS of neuropeptide knockdown males. *Myosuppressin* (**b**), *AT* (**c**), and *sNPFR* (**d**) knockdown males exhibited a minimum of 9, 6, and 7 RSs in 12 h, respectively. As a result, the durations of 9, 6, and 7 RSs are shown, respectively. Values are shown as mean \pm SEM, $n = 7-13$, two-way ANOVA with *post hoc* Šidák's multiple comparisons test, * $P < 0.05$, ** $P < 0.01$, *** $P < 0.001$. **e** Numbers of matings of male crickets injected with *dsDsRed*

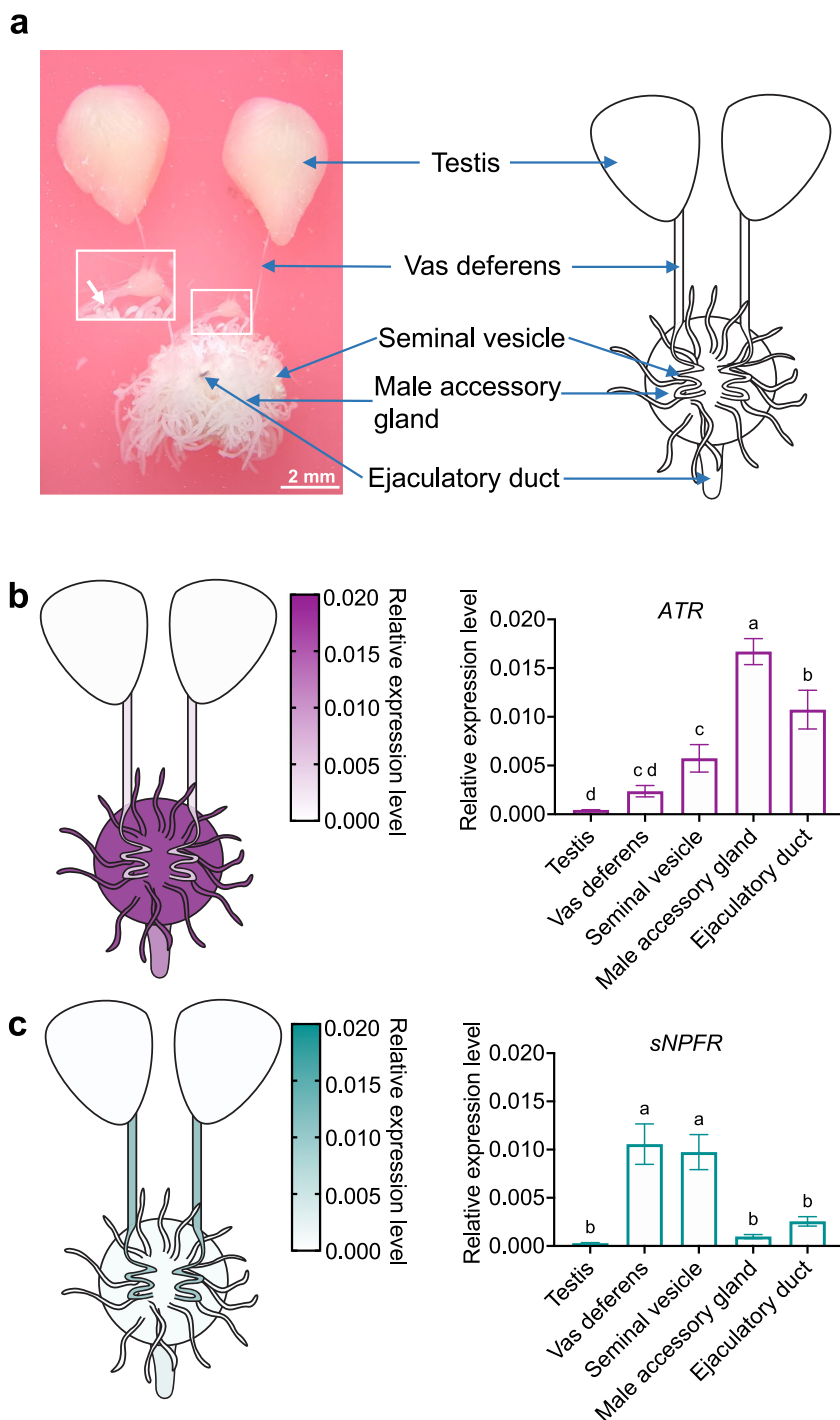
(*DsRed^{RNAi}*), *dsATR* (*ATR^{RNAi}*), or *dsNPFR* (*sNPFR^{RNAi}*) in 12 h. Values are shown as mean \pm SEM, $n = 8-9$, Dunnett's test, * $P < 0.05$. (**f**, **g**) Duration of each RS of receptor knockdown males. Both *ATR* (**f**) and *sNPFR* (**g**) knockdown males experienced 6 RSs in 12 h at least. The durations of 6 RSs are shown in these two graphs. Values are shown as mean \pm SEM, $n = 8-9$, two-way ANOVA with *post hoc* Šidák's multiple comparisons test, * $P < 0.05$, ** $P < 0.01$, **** $P < 0.0001$.

h Colocalization of AT peptide- and *sNPFR* mRNA-positive cells in the male TAG using immunohistochemistry and in situ hybridization. A dashed arrow points to AT peptide-specific positive cell cluster. Solid arrows point to *sNPFR* mRNA-specific positive cells. IR, immunoreactivity. Bar, 100 μ m.

Fig. 9a). When the final instar and adult stages were further divided into 5 periods, synchronically gradual increases were observed in the size of the MAG and the transcriptional levels of *AT* in the TAG, as well as *ATR* in the MAG (Supplementary Fig. 9b). These results indicated the intimate association between *AT* signaling pathway and MAG physiological activities. In contrast to the early emergence of MAG at the 3rd instar, the shaped SVs were absent until the third stage of the final instar (N3), when the terminals of vasa deferentia enlarged to form SVs. The SVs were empty at the final

instar, and progressively filled with spermatozoa after eclosion (Supplementary Fig. 9c). The transcriptional level of *sNPFR* in the male TAG remained constant during the final instar but progressively increased after eclosion. The *sNPFR* mRNA level was higher in sexually immature adults than that in the final instar nymphs; however, the transcriptional level was not altered after eclosion, irrespective of sexual maturation (Supplementary Fig. 9c), suggesting the presumable function of *sNPFR* signaling pathway in SV physiological activities after eclosion such as spermatozoon storage.

Fig. 6 | Different target sites of AT and sNPF within the male reproductive system. **a** Picture (left) and schematic diagram (right) of TAG-innervated male reproductive system in crickets. White box in the picture represents TAG innervation of male reproductive tissues which is enlarged. White arrow in the enlarged picture points toward the nerve projected from the TAG to the male accessory gland and seminal vesicle. **b, c** Left, the transcriptional levels of *ATR* (**b**) and *sNPF* (**c**) in the male reproductive system indicated by heatmap. Right, the transcriptional levels of *ATR* (**b**) and *sNPF* (**c**) examined by RT-qPCR. Values are shown as mean \pm SEM, $n = 5$, Tukey's test. Different letters represent significant differences.

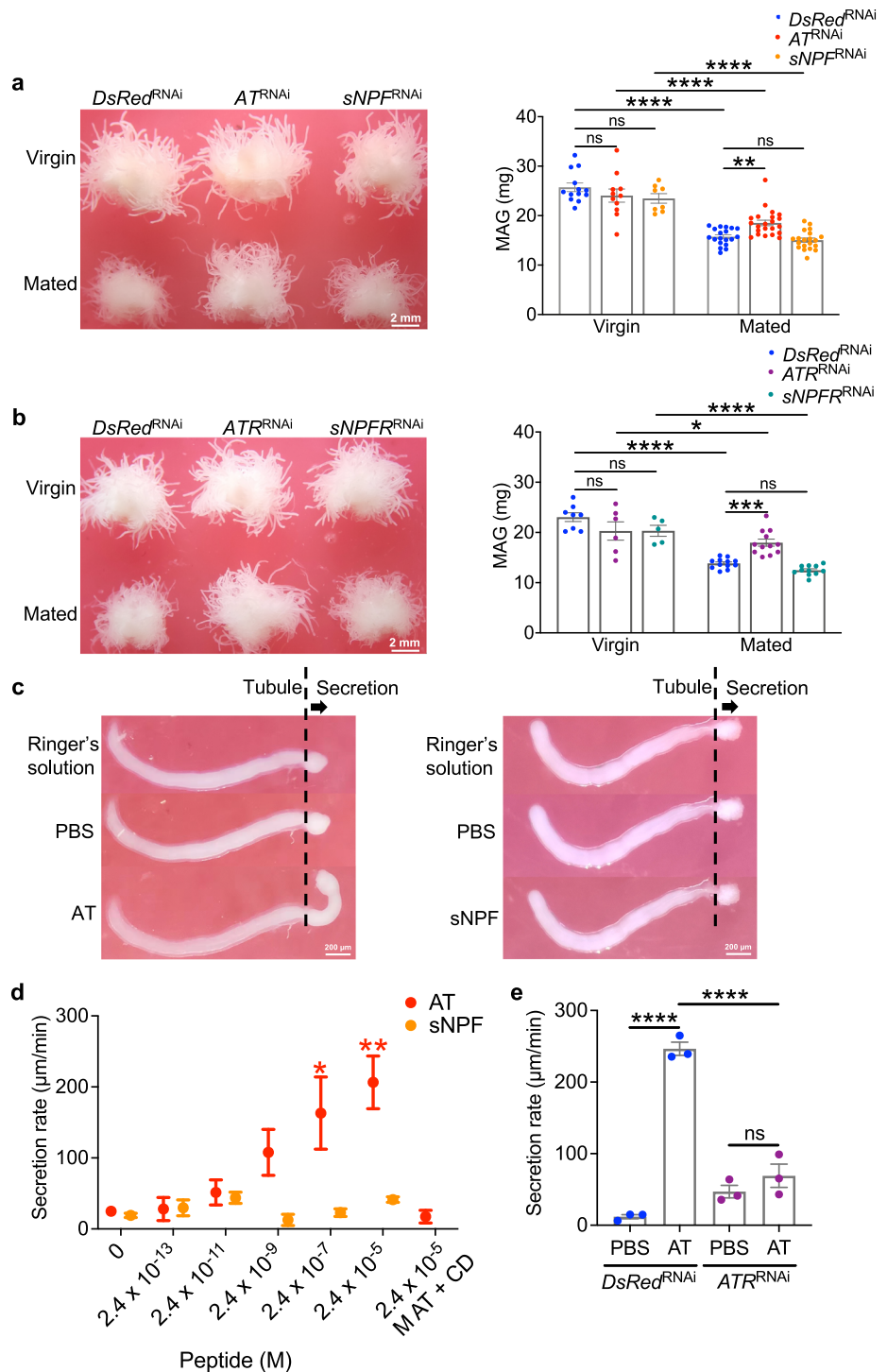


AT signaling pathway stimulates seminal fluid secretion from the male accessory gland

As *ATR* and *sNPF* were predominantly expressed in the MAG and SVs, respectively (Fig. 6), we delved into the specific roles of the two neuropeptide signaling pathways in the physiological activities in these tissues. Initially, we examined the impact of silencing *AT* and *sNPF* signaling pathways on the physiological activity of the MAG. The weight of MAG in *AT* and *ATR* knockdown virgin males was comparable to that in the control virgin males (Fig. 7a), suggesting that *AT* signaling pathway might not affect MAG growth. The MAG weight in males after successive matings for 24 h was much lower than that in the virgin males (Fig. 7a, b). We observed that the MAG tubules in the virgin *dsDsRed*-injected crickets were filled with milky seminal fluid, while the tubules in the mated *dsDsRed*-injected crickets were

almost transparent (Fig. 7a, b), suggesting that multiple matings results in secretion of a great amount of seminal fluid for spermatophore formation, as observed in stalk-eyed flies, *Cyrtodiopsis dalmanni*²⁹. The MAGs in *AT* knockdown crickets that underwent successive matings for 24 h were noticeably heavier than those in the control males (Fig. 7a). A similar effect was elicited by *ATR* knockdown (Fig. 7b). Considering the typical role of *AT* in the modulation of muscle contraction³⁰, the greater MAG weight in *AT* and *ATR* knockdown males after successive matings could be attributed to the inhibited MAG contraction, leading to the suppressed secretion of the MAG fluid. To verify this hypothesis, chemically synthesized *AT* was applied to the isolated MAG tubules immersed in Ringer's solution. Exposure to *AT* stimulated the secretion of tubular contents in a dose-dependent manner (Fig. 7c, d). *AT* at final concentrations of 24 μ M and

Fig. 7 | Regulation of MAG fluid secretion by neuropeptide signaling pathways. **a, b** Weight of MAGs dissected from *ATR* and *sNPFR* knockdown (**a**), or *ATR* and *sNPFR* knockdown (**b**) virgin and successively mated males. Left, pictures of MAGs. Right, quantification of the weight of MAGs. Virgin; males with sexual maturity but without mating experience. Mated; males that finished successively multiple matings for 24 h. Values are shown as mean \pm SEM, $n = 5-22$, Sidak's test for (**a, b**), $*P < 0.05$, $**P < 0.01$, $***P < 0.001$, $****P < 0.0001$. ns, not significant. **c** Pictures showing the isolated tubule with different treatments. **d** Effects of the synthetic AT and sNPF peptide application on the secretion of the fluid from the isolated MAG tubule and of cytochalasin D on the stimulatory effects of AT. Dashed lines represent the opening of the tubule. Arrows point to the direction of fluid secretion. Values are shown as mean \pm SEM, $n = 3$, Dunnett's test, $*P < 0.05$, $**P < 0.01$. ns not significant. **e** Effects of *ATR* knockdown on the stimulatory role of synthetic AT. Values are shown as mean \pm SEM, $n = 3$, Tukey's test, $****P < 0.0001$. ns not significant.



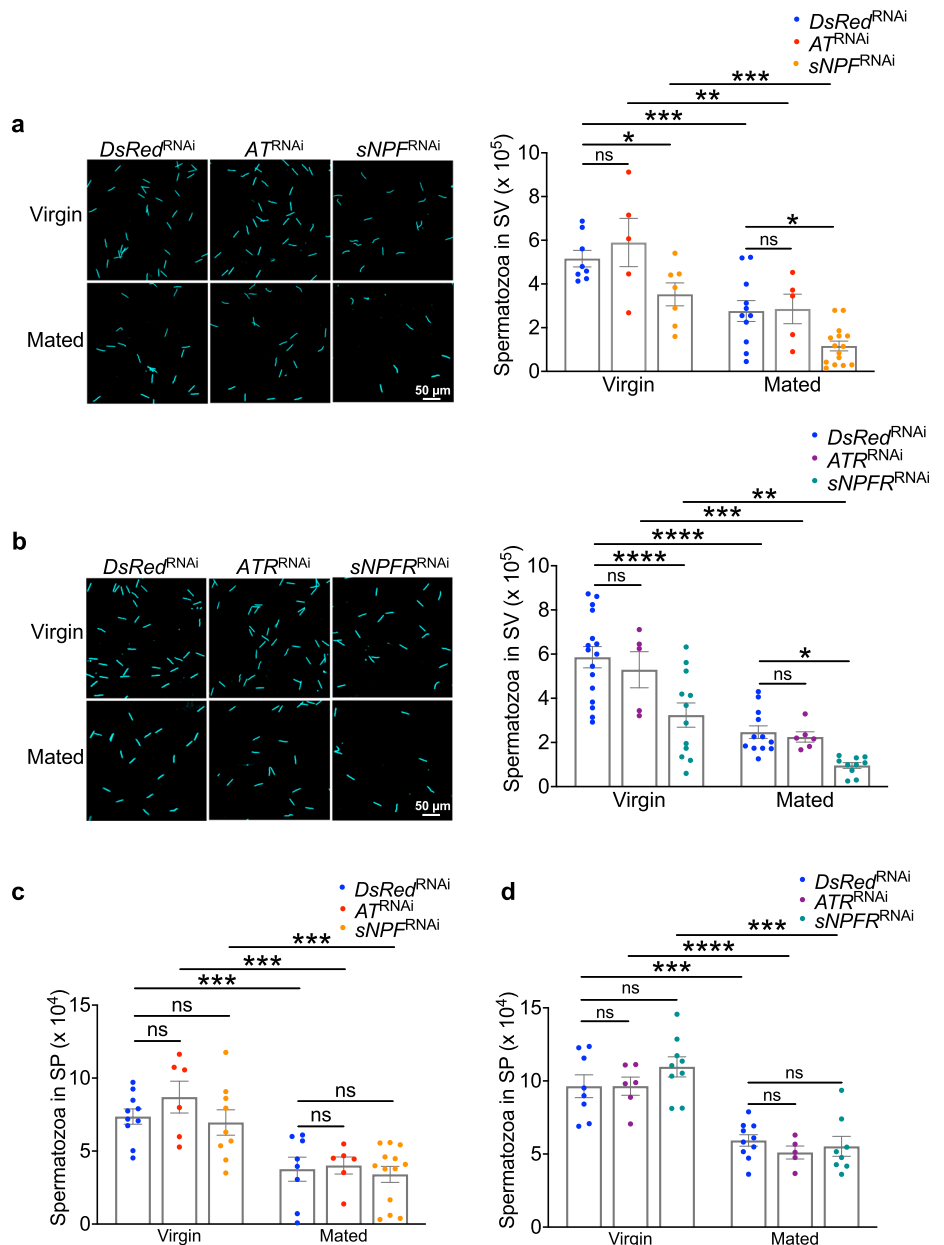
0.24 μM significantly increased the secretion (Fig. 7d), which was due to the noticeable contraction of the MAG tubule (Supplementary Movie 1). AT-immunoreactive nerve fibers were observed on the surface of the MAG tubule (Supplementary Fig. 8b). Furthermore, the contraction of the MAG tubules was impaired by *ATR* knockdown (Fig. 7e), suggesting that *ATR* mediates the AT-induced contraction of the MAG. It has been reported that there is fibrillar muscle surrounding the tubules in crickets²⁷. Cytochalasin D, an actin polymerization inhibitor, was applied to the tubule, which restrained the stimulatory effect of AT on the fluid secretion (Fig. 7d; Supplementary Movie 2), emphasizing the regulation of the MAG musculature by AT. In contrast, RNAi targeting *sNPFR* and *sNPFR* did not result

in any observable changes in the MAG size regardless of the cricket conditions (Fig. 7a, b). Moreover, exposure to sNPF peptide did not induce fluid secretion from MAG tubules (Fig. 7c, d). Consequently, AT, rather than sNPF signaling pathway, plays a crucial role in increasing seminal fluid secretion activity via stimulating muscle contraction of the MAG tubules.

sNPF signaling pathway promotes spermatozoon storage in seminal vesicles

The predominant distribution of *sNPFR* transcripts within the male reproductive system was observed in the vasa deferentia and SVs (Fig. 6c), indicating that sNPF signaling pathway may regulate spermatozoon

Fig. 8 | Regulation of spermatozoon storage in SVs by neuropeptide signaling pathways. a, b Effects of *AT* and *sNPf* knockdown (a), or *ATR* and *sNPFR* knockdown (b) on the number of spermatozoa in SVs of virgin and successively mated males. Left, fluorescent pictures of spermatozoa in seminal vesicles stained by DAPI. Right, quantification of spermatozoon counts. **c, d** Effects of *AT* and *sNPf* knockdown (c), or *ATR* and *sNPFR* knockdown (d) on the number of spermatozoa in spermatophores of virgin and successively mated males. Virgin; males with sexual maturity but without mating experience. Mated; males that have experienced successively multiple matings for 24 h. Values are shown as mean \pm SEM, $n = 5-16$, Sidak's test, * $P < 0.05$, ** $P < 0.01$, *** $P < 0.001$, **** $P < 0.0001$. ns not significant, SV seminal vesicle, SP spermatophore.



transport and storage. Like the seminal fluid in the MAG, the spermatozoa in the SVs were also reduced by successively multiple matings (Fig. 8a, b). Spermatozoa stored in the SVs were transported to form spermatophores. *sNPf* and *sNPFR* knockdown reduced the number of spermatozoa in the SVs of both virgin and successively mated males (Fig. 8a, b). To address whether the spermatozoon morphology was changed by the knockdown, we observed the shape by the differential interference contrast (DIC) images. The normal spermatozoa were composed of needle-shaped nuclei and extremely long tails. No abnormality in spermatozoon morphology was observed in the seminal vesicles of the knockdown males (Supplementary Fig. 10). The number of spermatozoa in spermatophores remained unaffected (Fig. 8c, d), indicating that *sNPf* signaling pathway promotes spermatozoon storage in the SVs but has no effect on the transport of spermatozoa from SVs to spermatophores. The lack of influence in the number of spermatozoa in SVs and spermatophores caused by *AT* and *ATR* knockdown suggests that the function of *sNPf* signaling pathway differs from that of *AT* signaling pathway (Fig. 8).

Successively multiple matings decreased the MAG weight and spermatozoon storage in the SVs (Figs. 7a, b, 8a, b). Given that the physiological

activities in the MAG and SVs were regulated by *AT*/*ATR* and *sNPf*/*sNPFR* signaling pathways (Figs. 7 and 8), the effects of multiple matings on the expression of *ATR* and *sNPFR* in these reproductive tissues were also examined. However, the male crickets with multiple matings displayed comparable transcriptional levels of *ATR* in the MAG and *sNPFR* in the SVs to the virgin males (Supplementary Fig. 6e, g)

sNPf signaling pathway in males regulates post-mating behaviors of females

MAG and SVs in males may produce special materials transferred to females to regulate post-mating behaviors in some insect species. Considering the effects of *AT* and *sNPf* signaling pathways on the MAG and SV functions, we evaluated the most typical post-mating behaviors, egg-laying and receptivity to remating, of females after mating with RNAi-treated males. The females mated with *AT* and *ATR* knockdown males laid comparable numbers of eggs with normal hatchability to the control and exhibited indistinguishable receptivity to another naïve virgin male (Fig. 9). In contrast, the post-mating behaviors of females were regulated by *sNPf* signaling pathway in males. Multiple matings had no effect on the

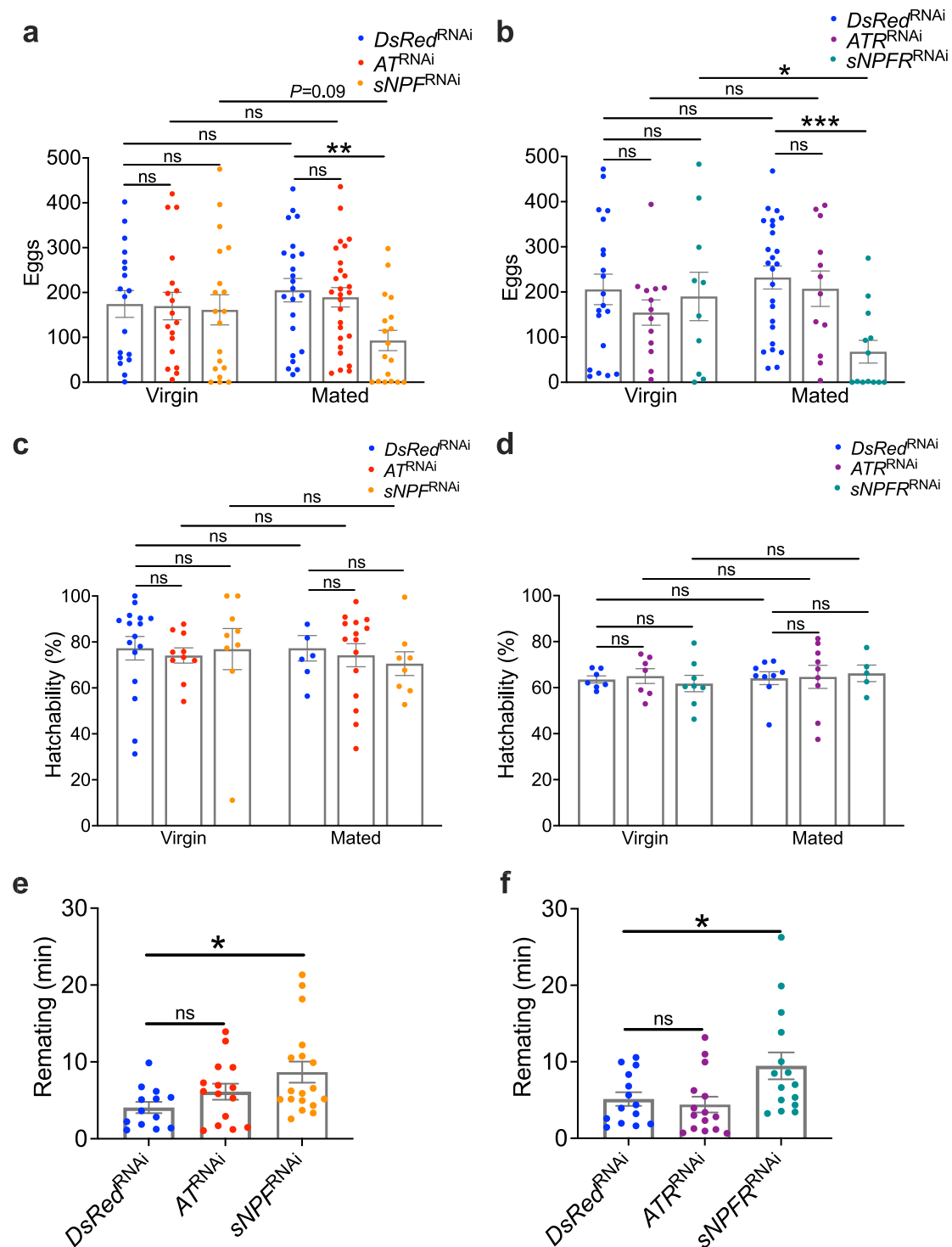


Fig. 9 | Regulation of post-mating behaviors of females by neuropeptide signaling pathways in males. a, b Effects of *AT* and *sNPF* knockdown (a), or *ATR* and *sNPFR* knockdown (b) in males on the number of eggs laid by the females during 24 h after mating with males. **c, d** Effects of *AT* and *sNPF* knockdown males (c), or *ATR* and *sNPFR* knockdown (d) on the hatchability of the eggs laid by the females. Values are

shown as mean \pm SEM, $n = 5-27$, Sidak's test, * $P < 0.05$, *** $P < 0.001$. ns not significant. SV, seminal vesicle. **e, f** Effects of *AT* and *sNPF* knockdown (e), or *ATR* and *sNPFR* knockdown (f) in males on the duration of remating of the mated females. Values are shown as mean \pm SEM, $n = 13-18$, Dunnett's test, * $P < 0.05$. ns not significant.

reproductive performance of *DsRed*, *AT*, and *ATR* knockdown males, as females that mated with the multiply mated males laid a similar number of eggs compared to the females that mated with the virgin males. In contrast, females that mated with *sNPF* knockdown males with multiple matings laid significantly fewer eggs compared to the females that mated with virgin

sNPFR knockdown males. A similar trend was observed in the case of *sNPF* knockdown males, suggesting that multiple matings reduced the fecundity of *sNPF* and *sNPFR* knockdown males (Fig. 9a, b). Although the number of spermatozoa transferred to females along with spermatophores was not affected by knocking down *sNPF* and *sNPFR* (Fig. 8c, d), the number of eggs

laid by the females mated with *sNPF* and *sNPFR* knockdown males that had experienced successively multiple matings was significantly reduced compared to the eggs laid by the females mated with the control males (Fig. 9a, b), while the hatchability was not influenced (Fig. 9c, d). These results confirmed the little relevance between the number of spermatozoa transferred to females along with spermatophores and the egg-laying behavior of females. Following successive matings with *sNPF* knockdown males for 24 h, the females took 8.7 min to complete a successful mating with another virgin male, significantly longer than the 4.1 min required by the females that had mated with the control males (Fig. 9e). Additionally, the females mated with *sNPFR* knockdown males exhibited took 9.5 min to remate, which was significantly longer than 5.1 min of the control (Fig. 9f). This suggests that the receptivity of females was reduced by silencing *sNPF* and *sNPFR*.

Discussion

This study demonstrated that four neuropeptides, *myosuppressin*, *AT*, *sNPF*, and *DH31* exhibited male-specific expression in the TAG based on in situ hybridization (Fig. 4). Of four peptides, *myosuppressin* knockdown had no effect on the post-mating refractoriness. *DH31* knockdown resulted in the failure of spermatophore transfer, preventing the completion of a mating. RNAi treatment resulted in a weak status of the crickets, decreasing the survival rate (Supplementary Fig. 2g). Probably due to the weakness, the male crickets with female mounting were unable to twist their body to hook the epiphallus onto the subgenital plate of females for spermatophore transfer³¹. A significant change was observed in the refractory stages of *AT* and *sNPF* knockdown male crickets (Fig. 5). *AT* and *sNPF* are pleiotropic neuropeptides in insects. Previous research on *AT* has predominantly focused on its regulatory roles in JH biosynthesis and muscle contraction³²; *sNPF* has been extensively studied for its involvement in feeding and metabolism³³. Several studies have hinted at the effects of *AT* and *sNPF* on oviposition in female insects^{34,35}. In contrast to these previous reports, our present study sheds light on the roles of *AT* and *sNPF* in the male-specific precisely timed post-mating refractoriness and the physiological activities in the male reproductive system, which have been much less studied so far.

The present study revealed that *AT* and *sNPF* knockdown significantly extended the post-mating RS (Fig. 5), suggesting that the two neuropeptides play crucial roles in promoting mating behavior and terminating the refractoriness. Knockdown of *AT* and *sNPF* might inhibit the restoration of sexual desire, thereby delaying the termination of the refractoriness. Nevertheless, it cannot be ruled out that the knockdown might attenuate male perception of females, as the attraction and stimulation from females are necessary to release refractoriness from a sexually responsive male¹¹. This is similar to the role of *ETH* in *Drosophila*, which modulates pheromone sensitivity to influence courtship behavior²². Our findings indicate that *AT* and *sNPF* may independently control the post-mating refractoriness through distinct downstream pathways (Supplementary Fig. 3). This contrasts with the functional interaction between the two neuropeptides reported in the silkworm, *Bombyx mori*, where *sNPF* enhances feeding motivation by counteracting the inhibitory effects of *AT*³⁶. Furthermore, in *B. mori*, *AT* from the brain stimulates the expression of *sNPF* in the corpora cardiaca to suppress JH synthesis in the corpora allata, specifically at the early 5th instar³⁷. These reports and the present work indicate that the functional interaction of *AT* and *sNPF* differs according to the species, tissues, and developmental stages.

The process of spermatophore preparation in the male reproductive system appears dispensable for maintaining the post-mating refractoriness, suggesting the independent regulation of the refractoriness and spermatophore preparation in crickets. Such independent regulation of the concurrently occurring reproductive behavior and reproductive physiological activity by the same factor is also reported in *D. melanogaster*. Four abdominal ganglion interneurons expressing a neuropeptide, *Corazonin*, in male fruit fly, independently control the copulation duration and the transfer of spermatozoa and seminal fluid³⁸. If the male reproductive system for spermatophore preparation does not mediate the effects of *AT* and *sNPF*

on the precisely timed refractoriness, there should be other target tissues of *AT* and *sNPF* by which the post-mating refractoriness is regulated. Brain is a potential target tissue since brain is the control center of stridulatory behavior in insects^{23–25}. A previous study suggests that TAG may secrete regulatory factors affecting the roles of brain in mating response during the RS in *G. bimaculatus*¹². It is speculated that *AT* and *sNPF* function as endocrinal regulatory factors that are secreted from the TAG to bind to their receptors in the brain to activate or inhibit downstream signaling, followed by initiation of courtship song and termination of the refractoriness. JH signaling can be excluded as the downstream of *AT* and *sNPF* in regulation of the refractoriness (Supplementary Fig. 5). Like crickets, male rat also exhibits post-mating refractoriness. Disruption of central serotonergic systems in the brain shortens the RS duration, whereas inhibition of central dopaminergic and noradrenergic systems increases the RS duration^{39–41}. Therefore, serotonin, dopamine, and octopamine, the monohydroxylic counterpart of noradrenaline in insects, presumably serve as the candidates of downstream molecules in the brain to mediate the effects of *AT* and *sNPF* signaling pathways on the refractoriness in crickets, which remains to be elucidated.

The distinguishable distributions of *ATR* and *sNPFR* in the male reproductive system highlight the distinct roles of the two neuropeptide signaling pathways in the physiological activities in the system. Silencing *AT* and *ATR* resulted in a greater MAG weight in crickets that had experienced multiple matings, attributed to the inhibited MAG tubule contraction that caused less fluid secretion (Fig. 7), which is reminiscent of the myostimulatory function of *AT* in other insect species^{42–44}. The reduced mating frequency, resulting in less usage of MAG fluid in *AT*/*ATR* knockdown males, could not account for the greater MAG weight because the successively mated *sNPF*/*sNPFR* knockdown males with lower mating frequency possessed MAGs with a comparable weight with the control (Fig. 7a, b). Knocking down *sNPF* signaling pathway in males had no effect on the MAG but reduced spermatozoon storage in the SVs (Fig. 8). This contrasts with the roles of *sNPF* in the male reproductive system of *Tenebrio molitor*, where the injection of *sNPF* peptide reduces spermatozoon number in the testes and vas deferens including SVs¹⁴. The species-dependent contrasting functions of *sNPF* are further exemplified by its ability to increase food intake in *D. melanogaster* while decreasing food intake in *Schistocerca gregaria*^{45,46}. These findings may reflect differences in *sNPF* function between holometabolous and hemimetabolous insects. Despite the reduced spermatozoon count in SVs, spermatozoon count in spermatophores was not altered. It is possible that the knockdown specifically affected the proportion of alive spermatozoa without altering the total spermatozoon count. Alternatively, while the knockdown reduced the overall spermatozoon count in the SVs, a sufficient number of spermatozoa could still remain to support some spermatophore formation. *sNPF* signaling pathway also contributed to the regulation of post-mating behaviors of females (Fig. 9). Although female crickets mated with *sNPF* and *sNPFR* knockdown males that had undergone multiple matings received spermatophores containing a normal number of spermatozoa, the females laid fewer eggs (Figs. 8c, d, 9a, b). SVs in males may produce a substance which functions like sex peptide, that is transferred to females together with spermatozoa in *D. melanogaster*⁵. This putative substance may regulate the post-mating behaviors of females, including egg-laying and receptivity to remating, and its production may be controlled by *sNPF* signaling pathway in male crickets.

AT and *sNPF* together regulated the duration of the post-mating refractoriness but modulated different functions of the male reproductive system (Figs. 5, 7, and 8). The regulation of these male-specific behavior and physiological activities by *AT* and *sNPF* in *G. bimaculatus* may be attributed to their male-specific expression in the male TAG (Fig. 4), which precisely controls the RS, and innervates the male reproductive system^{12,26}. *AT* and *sNPF* were colocalized in the large cells in the dorsal midline of the male TAG, with additional specific expression in different small cells (Fig. 5h). This suggests that the large cells co-expressing *AT* and *sNPF* may regulate

the post-mating refractoriness, while the smaller cells specifically expressing AT and sNPF may control the reproductive system; the group of small cells specifically expressing AT may regulate the seminal fluid secretion of MAG, whereas another two small cells specifically expressing sNPF may control the spermatozoon storage in SVs. Future work is needed to prove this hypothesis.

In summary, this study unveils the neuropeptide regulation of the post-mating refractoriness and physiological activities in the reproductive system in male crickets. AT and sNPF signaling pathways together regulate the duration of the post-mating refractoriness but influence different reproductive tissues. AT targets MAG, stimulating its seminal fluid secretion activity, while sNPF targets SVs, promoting spermatozoon storage in SVs, and affects the post-mating behaviors of females.

Methods

Insects

G. bimaculatus were reared in plastic containers (55 × 39 × 32 cm) at 28 ± 1 °C under a photoperiod of 16 h light and 8 h darkness. The diets were composed of rabbit food ORC4 (Orient Yeast, Tokyo, Japan) and cat food (Orient Yeast, Tokyo, Japan) at a weight ratio of 4:1.

RNA extraction and reverse transcription-quantitative PCR (RT-qPCR)

Tissues from crickets were isolated in saline solution (0.9% NaCl in distilled water) under the microscope. Total RNA was extracted using TRI reagent® (Molecular Research Center, Inc., Cincinnati, OH, USA) according to the manufacturer's protocol. The total RNA was treated with RQ DNase I (Promega Co., Madison, WI, USA) to remove the genomic DNA, followed by purification using phenol/chloroform extraction and ethanol precipitation. The purified RNA was dissolved in 0.1% diethylpyrocarbonate (DEPC)-treated water to a concentration of 100 ng µl⁻¹. The resulting RNA was reverse-transcribed to cDNA using ReverTra Ace® (Toyobo Co. Ltd., Osaka, Japan) for RT-qPCR. *G. bimaculatus elongation factor (EF)* (GenBank accession number: ABG01881.1) was used as the reference gene. The sizes of most amplified fragments were 60–100 bp with GC content of 40–60%. The mixture of the template cDNA, THUNDERBIRD® SYBR® qPCR Mix (Toyobo Co. Ltd.), and the primers for RT-qPCR (Table S1) was reacted on a Thermal Cycler Dice Real Time System TP850 (Takara, Shiga, Japan) with the program: 30 s at 95 °C, 40 cycles of 5 s at 95 °C, and 30 s at 60 °C; ended by a dissociation curve analysis at 95 °C for 15 s, at 60 °C for 30 s, and at 95 °C for 15 s. For the amplification of *kinin* fragment with 68% GC content, KOD SYBR® qPCR Mix (Toyobo Co. Ltd.) was used due to its relatively higher GC contents in the sequence. The experimental evaluation of RT-qPCR was performed by confirming the resulting dissociation curves. The relative transcriptional levels were calculated using 2^{-ΔCT} method⁴⁷.

Sampling from the crickets at different growth and development stages

Generally, crickets experience 8 or 9 nymphal instars and an adult stage. The crickets at different growth stages were divided into 5 groups (1st–2nd instar nymphs, 3rd–6th instar nymphs, penultimate instar nymphs, final instar nymphs and adults) based on the size and stage-specific morphological appearances (Supplementary Fig. 1). The external genitalia of females emerged at the 3rd instar. External wing pads emerged at the penultimate instar. The external genitalia and wing pads of the final instar nymphs became much longer than those of younger nymphs. Both sexes of the 1st and 2nd instar nymphs were mixed as one examining sample for RNA extraction because of their indistinguishable appearances (Supplementary Fig. 1).

RNA sequencing

Total RNA was extracted from the TAG of the male crickets on the fourth day after eclosion. RNA sequencing was performed using an Illumina NovaSeq 6000 platform with 100-bp paired-end reads by Macrogen Japan Corp. (Tokyo, Japan). It produced approximately 55 million paired reads. The processing and analysis of the sequencing results were conducted in

CLC Genomics Workbench 7.0 (<https://www.qiagenbioinformatics.com/>). The read sequences were submitted to NCBI (Accession: PRJNA1220312). Following assessing the quality of the raw reads, the adaptor sequences and low-quality reads were removed. The processed reads were then subjected to de novo assembly with parameters as follows: mismatch cost-2, insertion cost-3, deletion cost-3, length fraction-0.5, similarity-0.8, minimum contig length-200, kmer size-variable, bubble size-automatic. The assembly produced 171676 contigs.

The amino acid sequences of neuropeptides from other insects were downloaded from DiNER (<http://www.neurostresspep.eu/diner/infosearch>)⁴⁸ and used as queries for BLAST analysis to search for the homologous sequences in *G. bimaculatus*.

Whole-mount in situ hybridization

The primers for probe synthesis without T7 promoter (Table S1) were mixed with GoTaq® Master Mixes (Promega Co.) and TAG-derived cDNA to amplify fragments of cDNAs encoding neuropeptide precursors with sizes of 300–600 bp by PCR. The PCR products were purified using QIAquick Gel Extraction Kit (Qiagen, Hilden, Germany). The purified DNAs were inserted into pGEM-T vectors (Promega Co.) to construct cDNA-inserted plasmids, which were transformed into *Escherichia coli* to amplify. The forward primer without T7 promoter and the reverse primer with T7 promoter was used to amplify the target fragment from the cDNA-inserted plasmid. Then, the resulting PCR product served as the template, together with DIG RNA Labeling Mix (Roche, Mannheim, Germany) and T7 RNA Polymerase (Takara) to synthesize antisense RNA probes. The forward primer with T7 promoter and the reverse primer without T7 promoter were used for the synthesis of sense RNA probes, the negative control. TAGs were isolated from male and female adult crickets on the fourth day after eclosion and then fixed in 4% paraformaldehyde (PFA)/phosphate-buffered saline (PBS) at 4 °C overnight. After washing with PBS-0.1% Tween-20 (PBT), the TAGs were treated with proteinase K (5 µg ml⁻¹; Thermo Fisher Scientific, Waltham, MA, USA) for 10 min at room temperature and refixed using 0.2% glutaraldehyde in 4% PFA/PBS. The TAGs were next immersed in prehybridization buffer [50% formamide, 25% 20 × SSC, salmon sperm DNA (1 mg ml⁻¹; Thermo Fisher Scientific), heparin (1 mg ml⁻¹), 0.1% Tween-20] at 50 °C for 2 h, and then incubated in the hybridization solution (prehybridization buffer plus RNA probes at the final concentration of 1 ng µl⁻¹) at 50 °C for 16 h. Next, the washed samples were incubated with the anti-DIG-alkaline phosphatase (AP)-conjugated antibody (Roche) at 4 °C overnight. The samples were washed with staining buffer [Tris-HCl (100 mM, pH 8.8), NaCl (100 mM), MgCl₂ (50 mM), 0.1% Tween-20], and then added to nitroblue tetrazolium and bromo-chloro-indolyl-phosphate solution (NBT-BCIP, 1:50 in staining buffer, Roche) to develop color in the dark. The signal was detected under a microscope.

Chemical synthesis of neuropeptides

The amino acid sequences of mature AT and sNPF peptides are 'GFKNVALSTARGF-NH₂' and 'SNRSPSLRLRF-NH₂', respectively. The fluorenyl methoxycarbonyl (Fmoc) method was employed to synthesize the peptides as described previously with some modifications⁴⁹. Rink Amide resin (Sigma-Aldrich, St. Louis, MO, USA) was used to provide an amide to the C-terminal of the peptides. Fmoc amino acids (Kokusai Chemical, Tokyo, Japan) were coupled to the resin with the facilitation of 1-hydroxybenzotriazole and *N,N'*-dicyclohexylcarbodiimide in *N*-methylpyrrolidone. Before the addition of a new amino acid residue, the Fmoc protecting group of the previous amino acid was removed by 20% piperidine in dimethylformamide. After the elongation, the resin was removed by treatment with a mixture of trifluoroacetic acid (TFA), dichloromethane, anisole, trimethylsilyl bromide, and 3,4-ethoxylene dioxothiophene with a volume ratio of 10:5:2:2:1 on ice for 1 h. The resulting peptides were mixed with diethyl ether and centrifuged for precipitation. The precipitants were dissolved in 0.1% TFA aqueous solution and desalted using a reversed-phase Sep-Pak® C18 cartridge (Waters Co., Milford, MA, USA), and then the peptide fraction was eluted with 60% acetonitrile in 0.1% TFA aqueous

solution. The eluate was purified using a reversed-phase high-performance liquid chromatography (HPLC) (Jasco SC-802, PU-880, UV-875; Jasco Int., Tokyo, Japan) on a Senshu Pak PEGASIL-300 ODS column (4.6 mm i.d. × 250 mm; Senshu Kagaku, Tokyo, Japan) with a linear gradient of 0–60% acetonitrile in 0.1% TFA over 40 min at the flow rate of 1 ml min⁻¹. The chromatography was monitored by 225 nm. The purified synthetic AT and sNPF were confirmed by measurement with MALDI-TOF MS analysis using TOF/TOF 5800 System (AB SCIEX, Framingham, MA, USA). The measurement was carried out in the positive reflector mode with an accelerating voltage of 30 kV. The mixture of the purified sample solution (1 µl) and the saturated solution (1 µl) of α-cyano-4-hydroxycinnamic acid (Sigma-Aldrich) in 60% acetonitrile/0.1% TFA was loaded on the target plate for the measurement of AT peptide (a theoretical *m/z* 1366.6) and sNPF peptide (a theoretical *m/z* 1331.8). The purified peptides were lyophilized and then dissolved in PBS.

Antibody characterization

The polyclonal rabbit antiserum (Eurofins Genomics K.K., Tokyo, Japan) was generated against AT peptide with the sequence 'NH₂-C + GFKNVALSTARGF-CONH₂'. The specificity of AT antiserum was tested by a dot-immunoblotting assay as previously described with slight modifications^{50,51}. PVDF membrane (Hybond-P; Amersham, Buckinghamshire, UK) was first rinsed in methanol and subsequently rinsed in water for hydration. One microliter of chemically synthetic AT and sNPF with different concentrations dissolved in water was dotted on the PVDF membrane, followed by air-drying. Non-specific sites were blocked by soaking the membrane in Tris-buffered saline (pH 7.5)-0.1% Tween containing 5% skim milk (TBSTS) for 1 h. The membrane was then incubated with an AT antiserum (1:1000) in TBSTS for 1 h. After washing with TBST three times, the membrane was incubated with the horseradish peroxidase-conjugated secondary antibody (1:3000; Invitrogen, MA, USA) in TBST for 1 h. A chemiluminescence reaction kit (ImmunoStar LD; Wako, Osaka, Japan) was used to develop the signals. The result revealed that the addition of AT, but not sNPF peptide, produced a signal, indicating AT-antibody binding. The intensity of the spots decreased with reducing concentrations of AT peptides and the antiserum (Supplementary Fig. 7a).

The antiserum specificity was further validated using a preadsorption assay^{52,53}. For immunostaining, TAGs were dissected and fixed in 4% PFA at 4 °C overnight. The TAGs were then washed with PBS containing 0.5% TritonX-100 (PBSTr) and blocked at room temperature for 1 h using blocking buffer [10% goat serum (Invitrogen), 2% BSA (Wako), 0.5% TritonX-100]. AT was added to the blocking buffer containing the antiserum (1:1000) to achieve final concentrations of 73, 7.3, and 0.73 µM. The mixture was incubated at 4 °C for 24 h, followed by centrifugation at 15000 rpm for 30 min. The supernatants, along with the untreated antiserum and pre-immune serum, were used to incubate the TAGs at 4 °C overnight. After washing with PBSTr, the TAGs were incubated with the goat anti-rabbit IgG labeled with Alexa 488 (1:1000; Invitrogen) at room temperature for 2 h, and then mounted with 50% glycerol/PBS. The signal was visualized using an FV3000 confocal laser scanning microscope (Olympus, Tokyo, Japan). The immunoactivity of AT was completely abolished by antiserum preadsorption with 73, 7.3, and 0.73 µM AT (Supplementary Fig. 7b).

Furthermore, the antiserum specificity was confirmed using double staining of AT peptide and AT mRNA. Whole-mount in situ hybridization and immunohistochemistry were performed to detect the colocalization. Following hybridization with the RNA probe, the tissues were incubated with an anti-DIG-AP-conjugated antibody (1:1000) together with the rabbit antiserum against AT (1:1000) at 4 °C overnight. The color of the signal for in situ hybridization was developed using Fast Red (Sigma-Aldrich) and checked under the microscope every half an hour to avoid overstaining. After washing with PBSTr, the tissues were incubated with the secondary antibody labeled with Alexa 488 at room temperature for 2 h. The signal detection was performed using a confocal microscope. The equivalent signals were obtained using immunohistochemistry for AT peptide and in situ hybridization for AT mRNA (Supplementary Fig. 7c).

RNA interference

The knockdown-targeting cDNA fragments ranging from 300–600 bp were amplified by PCR using the cDNA-inserted plasmids. The primers used for PCR had a T7 sequence at the 5' end, as listed in Table S1. The double-stranded RNA (dsRNA) was synthesized using T7 RNA Polymerase (Takara). The resulting dsRNA (10 µg) was injected into the abdomen of the final instar male crickets just after penultimate molting. All crickets finished the final molting to become adults successfully, confirming that there was no developmental deficit caused by RNAi. Partial sequence encoding *Discosoma sp.* red fluorescent protein (*DsRed*; GenBank accession number: AAT48428.1) was used as a control for RNAi experiments in this study. The RNAi-treated crickets underwent the final instar stage, which lasted approximately one week⁵⁴. Four days after eclosion, when the crickets became sexually mature, they were subjected to RNAi efficiency examination. *DH31* knockdown males appeared weak. Their survival rate was significantly reduced after 30 days of dsRNA injection compared to the control (Supplementary Fig. 2g). RNAi targeting *myosuppressin*, *AT*, and *sNPF* did not cause mortality (Supplementary Fig. 2h), minimizing the possibility of side effects of RNAi on mating behavior.

Mating assays

Sexually matured crickets around one week after eclosion were used. To illuminate the effects of RNAi on RS duration, each dsRNA-injected male cricket was paired with 3 virgin females to reduce the influence of female refractoriness on the mating success by males during 12 h. The duration of RS was measured by observation on video-recorded crickets. The duration of total RS but not the separated RS1 and RS2 was measured because of the continuous physical and physiological stimulation from the accompanied females in the same container, ensuring the appropriately fixed RS1 and RS2 duration.

To study the post-mating behaviors of the females, each RNAi-treated male cricket was mated with a virgin female. After once mating, the mated females were reared individually in a plastic container with freely available food and water-soaked tissue for water supply as well as for oviposition. The number of eggs laid by females during the next 24 h was counted. The water-soaked tissue was placed in a new container. The number of hatched nymphs was counted for the calculation of hatchability. To investigate the female receptivity, each female that had been paired with an RNAi-treated male for 24 h was mated with a virgin male without any treatment. The duration of remating, from the initiation of male courtship to the dismounting of females with an attached spermatophore in the genitalia opening⁵⁵, was recorded to assess the receptivity.

MAG secretion assay

MAG secretion assay was performed as previously described²⁷. MAGs were isolated from sexually matured virgin adult males about one week after eclosion. The tubule of MAG was cut at the base. The isolated tubule was immersed in 10 µl of Ringer's solution [NaCl (140 mM), KCl (4.7 mM), CaCl₂ (2 mM), MgCl₂ (2 mM), HEPES-NaOH (5 mM, pH 7.1)]. First, PBS (10 µl) was applied to the tubule. After 1 min, the synthetic AT or sNPF in PBS (10 µl) was applied to the tubule. The secretion rate was determined by measuring the length of secreted fluid over 1 min as the secreted fluid volume is approximately proportional to the secreted fluid length. The difference before and after addition of PBS was calculated as the control. The difference before and after addition of the synthetic neuropeptides was calculated as the secretion activity. To investigate the effects of cytochalasin D on the muscle contraction of MAG tubule, the isolated tubule was immersed in 100 µM cytochalasin D (Cayman Chemical, Ann Arbor, MI, USA) diluted in Ringer's solution, followed by the application of PBS and neuropeptide.

Spermatozoon counts

Spermatozoa were counted as described previously with some modifications⁵⁶. Seminal vesicles and spermatophores were isolated from virgin and successively mated males in saline solution and then transferred

to PBS (1 ml and 100 µl, respectively). The spermatozoa were released from the tissues by sonication. One microliter of the sperm-suspended solution was loaded on a slide and air-dried. The spermatozoon spot was then covered with 4% PFA/PBS and air-dried, followed by addition of 90% ethanol and air-drying. The spermatozoon DNA was stained with DAPI (1 µg ml⁻¹; Wako) in PBS at room temperature for 30 min. After washing with PBS, 50% glycerol/PBS was added to the slide which was then covered with a coverslip. The spermatozoa counts were measured under the fluorescence microscope.

For the observation of spermatozoon morphology, the seminal vesicles were dissected from virgin and mated RNAi male crickets on the fourth day after eclosion and then loaded on a slide, which was imaged under a microscope using DIC optics.

Statistics and reproducibility

Data plotting and statistical analyses were performed using GraphPad Prism. Schematic diagrams were drawn using Adobe Illustrator. All the experiments in the figures were performed at least twice. The statistical analyses were described in the respective figure legends.

Reporting summary

Further information on research design is available in the Nature Portfolio Reporting Summary linked to this article.

Data availability

The source data behind the graphs in the paper are at following accession number (<https://doi.org/10.5061/dryad.vhhmgqp1x>).

Received: 14 November 2024; Accepted: 13 May 2025;

Published online: 11 June 2025

References

- Ridley, M. Mating frequency and fecundity in insects. *Biol. Rev.* **63**, 509–549 (1988).
- Walker, W. F. Sperm utilization strategies in non-social insects. *Am. Nat.* **115**, 780–799 (1980).
- Sakaluk, S. K. & Cade, W. H. Female mating frequency and progeny production in singly and doubly mated house and field cricket. *Can. J. Zool.* **58**, 404–411 (1980).
- Parker, G. A. Sperm competition and its evolution consequences in the insects. *Biol. Rev.* **45**, 525–567 (1970).
- Chapman, T. et al. The sex peptide of *Drosophila melanogaster*: Female post-mating responses analyzed by using RNA interference. *Proc. Natl Acad. Sci. USA*. **100**, 9923–9928 (2003).
- Peng, D. et al. A male steroid controls female sexual behaviour in the malaria mosquito. *Nature* **608**, 93–97 (2022).
- Ureshi, M. & Sakai, M. Location of the reproductive timer in the male cricket *Gryllus bimaculatus* DeGeer as revealed by local cooling of the central nervous system. *J. Comp. Physiol. A*. **186**, 1159–1170 (2001).
- Fleischman, R. & Sakaluk, S. Sexual conflict over remating in house crickets: no evidence of an anti-aphrodisiac in males' Ejaculates. *Behav* **141**, 633–646 (2004).
- Loher, W. & Rence, B. The mating behavior of *Teleogryllus commodus* (Walker) and its central and peripheral control. *Z. für Tierpsychologie* **46**, 225–259 (2010).
- Sakai, M., Taoda, Y., Mori, K., Fujino, M. & Ohta, C. Copulation sequence and mating termination in the male cricket *Gryllus bimaculatus* DeGeer. *J. Insect Physiol.* **37**, 599–615 (1991).
- Nagao, T. & Shimozaawa, T. A fixed time-interval between two behavioural elements in the mating behaviour of male crickets, *Gryllus bimaculatus*. *Anim. Behav.* **35**, 122–130 (1987).
- Sakai, M., Matsumoto, Y., Takemori, N. & Taoda, Y. Post-copulatory sexual refractoriness is maintained under the control of the terminal abdominal ganglion in the male cricket *Gryllus bimaculatus* DeGeer. *J. Insect Physiol.* **41**, 1055–1070 (1995).
- Schoofs, L., De Loof, A. & Van Hiel, M. B. Neuropeptides as regulators of behavior in insects. *Ann. Rev. Entomol.* **62**, 35–52 (2017).
- Marciniak, P. et al. Short neuropeptide F signaling regulates functioning of male reproductive system in *Tenebrio molitor* beetle. *J. Comp. Physiol. B* **190**, 521–534 (2020).
- Gong, W. et al. Neuropeptide natalisin regulates reproductive behaviors in *Spodoptera frugiperda*. *Sci. Rep.* **14**, 15122 (2024).
- Lange, A. B., Kisana, A., Leyria, J. & Orchard, I. The male reproductive system of the kissing bug, *Rhodnius prolixus* Stål, 1859 (Hemiptera: Reduviidae: Triatominae): Arrangements of the muscles and the myoactivity of the selected neuropeptides. *Insects* **14**, 324 (2023).
- Rankin, S. M., TeBrugge, V. A., Murray, J. A., Schuler, A. M. & Tobe, S. S. Effects of selected neuropeptides, mating status and castration on male reproductive tract movements and immunolocalization of neuropeptides in earwigs. *Comp. Biochem. Physiol. A Mol. Integr. Physiol.* **152**, 83–90 (2009).
- Cheng, J. et al. Corazonin signaling modulates the synthetic activity of male accessory gland in *Grapholita molesta*. *Int. J. Biol. Macromol.* **216**, 446–455 (2022).
- Kumashiro, M. & Sakai, M. Genital autocleaning in the male cricket *Gryllus bimaculatus* (1): Structure and function of the genital membrane. *Zool. Sci.* **33**, 623–633 (2016).
- Brent, C. S. Reproductive refractoriness in the western tarnished plant bug (Hemiptera: Miridae). *Ann. Entomol. Soc. Am.* **103**, 300–306 (2010).
- Thornhill, R. & Alcock, J. *The evolution of insect mating systems*. (Harvard University of Press, 1983).
- Meiselman, M. R., Ganguly, A., Dahanukar, A. & Adams, M. E. Endocrine modulation of primary chemosensory neurons regulates *Drosophila* courtship behavior. *PLoS Genet* **18**, e1010357 (2022).
- Hedwig, B. A descending brain neuron elicits stridulation in the cricket *Gryllus bimaculatus* (de Geer). *Naturwissenschaften* **83**, 428–429 (1996).
- Wenzel, B. & Hedwig, B. Neurochemical control of cricket stridulation revealed by pharmacological microinjections into the brain. *J. Exp. Biol.* **202**, 2203–2216 (1999).
- Huber, F. The role of the central nervous system in Orthoptera during the co-ordination and control of stridulation. *Z. vergl. Physiol* **44**, 60–132 (1963).
- Yamaguchi, T., Kushiro, N. & Waki, T. Sexual dimorphism of the terminal abdominal ganglion of the cricket. *Naturwissenschaften* **72**, 153–154 (1985).
- Kimura, T., Yasuyama, K. & Yamaguchi, T. Proctolinergic innervation of the accessory gland in male crickets (*Gryllus bimaculatus*): Detection of proctolin and some pharmacological properties of myogenically and neurogenically evoked contractions. *J. Insect Physiol.* **35**, 251–264 (1989).
- Čížmár, D., Roller, L., Pillerová, M., Sláma, K. & Žitňan, D. Multiple neuropeptides produced by sex-specific neurons control activity of the male accessory glands and gonoducts in the silkworm *Bombyx mori*. *Sci. Rep.* **9**, 2253 (2019).
- Rogers, D. W., Chapman, T., Fowler, K. & Pomiankowski, A. Mating-induced reduction in accessory reproductive organ size in the stalk-eyed fly *Cyrtodiopsis dalmanni*. *BMC Evol. Biol.* **5**, 37 (2005).
- Mizoguchi, A. Allatotropin in *Handbook of Hormones* 412–e57-1 (Elsevier, 2016).
- Sakai, M. & Kumashiro, M. Copulation in the cricket is performed by chain reaction. *Zool. Sci.* **21**, 705–718 (2004).
- Elekonich, M. M. & Horodyski, F. M. Insect allatotropins belong to a family of structurally-related myoactive peptides present in several invertebrate phyla. *Peptides* **24**, 1623–1632 (2003).
- Fadda, M. et al. Regulation of feeding and metabolism by neuropeptide F and short neuropeptide F in invertebrates. *Front. Endocrinol.* **10**, 64 (2019).

34. Hassanien, I. T. E., Meyering-Vos, M. & Hoffmann, K. H. RNA interference reveals allatotropin functioning in larvae and adults of *Spodoptera frugiperda* (Lepidoptera, Noctuidae). *Entomologia* **2**, 169 (2014).
35. Peng, X. et al. Expression patterns and functional analysis of the short neuropeptide F and NPF receptor genes in *Rhopalosiphum padi*. *Insect Sci.* **28**, 952–964 (2021).
36. Matsumoto, S. et al. Antagonistic effect of short neuropeptide F on allatotropin-inhibited feeding motivation of the silkworm larva, *Bombyx mori*. *Zool. Sci.* **36**, 58 (2019).
37. Kaneko, Y. & Hiruma, K. Short neuropeptide F (sNPF) is a stage-specific suppressor for juvenile hormone biosynthesis by corpora allata, and a critical factor for the initiation of insect metamorphosis. *Dev. Biol.* **393**, 312–319 (2014).
38. Tayler, T. D., Pacheco, D. A., Hergarden, A. C., Murthy, M. & Anderson, D. J. A neuropeptide circuit that coordinates sperm transfer and copulation duration in *Drosophila*. *Proc. Natl Acad. Sci. U.S.A.* **109**, 20697–20702 (2012).
39. McIntosh, T. K. & Barfield, R. J. Brain monoaminergic control of male reproductive behavior. I. Serotonin and the post-ejaculatory refractory period. *Behav. Brain Res.* **12**, 255–265 (1984).
40. McIntosh, T. K. & Barfield, R. J. Brain monoaminergic control of male reproductive behavior. II. Dopamine and the post-ejaculatory refractory period. *Behav. Brain Res.* **12**, 267–273 (1984).
41. McIntosh, T. K. & Barfield, R. J. Brain monoaminergic control of male reproductive behavior. III. Norepinephrine and the post-ejaculatory refractory period. *Behav. Brain Res.* **12**, 275–281 (1984).
42. Duve, H., East, P. D. & Thorpe, A. Regulation of lepidopteran foregut movement by allatostatins and allatotropin from the frontal ganglion. *J. Comp. Neurol.* **413**, 405–416 (1999).
43. Matthews, H. J., Audsley, N. & Weaver, R. J. Interactions between allatostatins and allatotropin on spontaneous contractions of the foregut of larval *Lacanobia oleracea*. *J. Insect Physiol.* **53**, 75–83 (2007).
44. Villalobos-Sambucaro, M. J. et al. Allatotropin modulates myostimulatory and cardioacceleratory activities in *Rhodnius prolixus* (Stal). *PLoS ONE* **10**, e0124131 (2015).
45. Dillen, S., Verdonck, R., Zels, S., Van Wielendaele, P. & Vanden Broeck, J. Identification of the short neuropeptide F precursor in the desert locust: Evidence for an inhibitory role of sNPF in the control of feeding. *Peptides* **53**, 134–139 (2014).
46. Lee, K. S., You, K. H., Choo, J. K., Han, Y. M. & Yu, K. *Drosophila* short neuropeptide F regulates food intake and body size. *J. Biol. Chem.* **279**, 50781–50789 (2004).
47. Konuma, T., Tsukamoto, Y., Nagasawa, H. & Nagata, S. Imbalanced hemolymph lipid levels affect feeding motivation in the two-spotted cricket, *Gryllus bimaculatus*. *PLoS ONE* **11**, e0154841 (2016).
48. Yeoh, J. G. C. et al. DIneR: Database for insect neuropeptide research. *Insect Biochem. Mol. Biol.* **86**, 9–19 (2017).
49. Zhou, Y. J., Fukumura, K. & Nagata, S. Effects of adipokinetic hormone and its related peptide on maintaining hemolymph carbohydrate and lipid levels in the two-spotted cricket, *Gryllus bimaculatus*. *Biosci. biotechnol. biochem.* **82**, 274–284 (2018).
50. Sato, Y., Shiomi, K., Saito, H., Imai, K. & Yamashita, O. Phe-X-Pro-Arg-Leu-NH₂ peptide producing cells in the central nervous system of the silkworm, *Bombyx mori*. *J. Insect Physiol.* **44**, 333–342 (1998).
51. Sun, J. S. et al. Developmental expression of FXPRLamide neuropeptides in peptidergic neurosecretory cells of diapause- and nondiapause-destined individuals of the cotton bollworm, *Helicoverpa armigera*. *Gen. Comp. Endocrinol.* **141**, 48–57 (2005).
52. Homberg, U., Vitzthum, H., Müller, M. & Binkle, U. Immunocytochemistry of GABA in the central complex of the locust *Schistocerca gregaria*: Identification of immunoreactive neurons and colocalization with neuropeptides. *J. Comp. Neurol.* **409**, 495–507 (1999).
53. Yamanaka, N. et al. *Bombyx* orckokinins are brain-gut peptides involved in the neuronal regulation of ecdysteroidogenesis. *J. Comp. Neurol.* **519**, 238–246 (2011).
54. Zhu, Z. & Nagata, S. Ion transport peptide and ion transport peptide-like regulate ecdysis behavior and water transport during ecdysis in *Gryllus bimaculatus*. *Insect Biochem. Mol. Biol.* **173**, 104178 (2024).
55. Gordon, D. G., Gershman, S. N. & Sakaluk, S. K. Glycine in nuptial food gifts of decorated crickets decreases female sexual receptivity when ingested, but not when injected. *Ani. Behav.* **83**, 369–375 (2012).
56. Bredlau, J. P., El-Sabrou, A. M. & Bressac, C. Reproductive context of extremely short sperm in the parasitic wasp *Cotesia congregata* (Hymenoptera: Braconidae). *Biol. J. Linn. Soc. Lond.* **131**, 384–395 (2020).

Acknowledgements

This work is partly supported by Grants-in-Aid for Scientific Research, KAKENHI, Grant Numbers 19H02967, 20K21304, and 21H02129.

Author contributions

Z.Z. and S.N. designed this experimental project. Z.Z. performed all experiments, analyzed the data, and wrote the initial draft of the manuscript. S.N. supervised the study and co-wrote the paper. Z.Z. and S.N. discussed the results and reviewed the manuscript.

Competing interests

The authors declare no competing interests.

Additional information

Supplementary information The online version contains supplementary material available at <https://doi.org/10.1038/s42003-025-08219-0>.

Correspondence and requests for materials should be addressed to Shinji Nagata.

Peer review information *Communications Biology* thanks Jean-Paul Paluzzi and the other, anonymous, reviewers for their contribution to the peer review of this work. Primary Handling Editors: Frank Avila and Benjamin Bessieres. A peer review file is available.

Reprints and permissions information is available at <http://www.nature.com/reprints>

Publisher's note Springer Nature remains neutral with regard to jurisdictional claims in published maps and institutional affiliations.

Open Access This article is licensed under a Creative Commons Attribution-NonCommercial-NoDerivatives 4.0 International License, which permits any non-commercial use, sharing, distribution and reproduction in any medium or format, as long as you give appropriate credit to the original author(s) and the source, provide a link to the Creative Commons licence, and indicate if you modified the licensed material. You do not have permission under this licence to share adapted material derived from this article or parts of it. The images or other third party material in this article are included in the article's Creative Commons licence, unless indicated otherwise in a credit line to the material. If material is not included in the article's Creative Commons licence and your intended use is not permitted by statutory regulation or exceeds the permitted use, you will need to obtain permission directly from the copyright holder. To view a copy of this licence, visit <http://creativecommons.org/licenses/by-nc-nd/4.0/>.

© The Author(s) 2025